

# Electropolymerization on Microelectrodes: Functionalization Technique for Selective Protein and DNA Conjugation

Eric Stern,<sup>\*†</sup> Steven Jay,<sup>†‡</sup> James Bertram,<sup>†‡</sup> Benjamin Boese,<sup>§</sup> Ilona Kretzschmar,<sup>||</sup> Daniel Turner-Evans,<sup>⊥</sup> Carl Dietz,<sup>⊥</sup> David A. LaVan,<sup>#</sup> Tadeusz Malinski,<sup>◇</sup> Tarek Fahmy,<sup>†</sup> and Mark A. Reed<sup>⊥,☆</sup>

Departments of Biomedical Engineering, Chemical Engineering, Applied Physics, Mechanical Engineering, and Electrical Engineering, Yale University, P.O. Box 208248, New Haven, Connecticut 06520, Department of Chemical Engineering, The City College of New York, 138th Street at Convent Avenue, New York, New York 10031, and Department of Biochemistry, Ohio University, 350 West State Street, Athens, Ohio 45701

A critical shortcoming of current surface functionalization schemes is their inability to selectively coat patterned substrates at micrometer and nanometer scales. This limitation prevents localized deposition of macromolecules at high densities, thereby restricting the versatility of the surface. A new approach for functionalizing lithographically patterned substrates that eliminates the need for alignment and, thus, is scalable to any dimension is reported. We show, for the first time, that electropolymerization of derivatized phenols can functionalize patterned surfaces with amine, aldehyde, and carboxylic acid groups and demonstrate that these derivatized groups can covalently bind molecular targets, including proteins and DNA. With this approach, electrically conducting and semiconducting materials in any lithographically realizable geometry can be selectively functionalized, allowing for the sequential deposition of a myriad of chemical or biochemical species of interest at high density to a surface with minimal cross-contamination.

There is an ever-increasing demand for the selective placement of functional molecules with micrometer to nanometer accuracy for sensing, assaying, and signaling applications. The key limitation is that current chemical and biochemical deposition schemes have not kept pace with the precision attainable by both traditional lithography<sup>1</sup> and nanotube and nanowire schemes.<sup>2,3</sup> A method that allows selective functionalization of micro- and nanoscale electronic devices would enable multiple potential functions at very high densities on a single surface and would have implications in

many fields, including DNA and protein microarrays,<sup>4,5</sup> nanowire and nanotube sensors,<sup>6</sup> lab-on-a-chip platforms,<sup>7</sup> drug discovery platforms,<sup>8</sup> and drug delivery systems.<sup>9</sup>

To achieve selective functionalization, we utilize the method of phenol electropolymerization, which has been previously shown to deposit insulating films on Pt wires,<sup>10–16</sup> primarily for the development of amperometric and potentiometric sensors. Electropolymerization is a process whereby a conducting<sup>17–25</sup> or insulat-

\* To whom correspondence should be addressed. E-mail: Eric.Stern@Yale.edu.

† Department of Biomedical Engineering, Yale University.

‡ These authors contributed equally to this work.

§ Chemical Engineering, Yale University.

|| The City College of New York.

⊥ Applied Physics, Yale University.

# Mechanical Engineering, Yale University.

◇ Ohio University.

☆ Electrical Engineering, Yale University.

(1) ITRS Semiconductor Roadmap: <http://public.itrs.net/>.

(2) Wang, J. *Electroanalysis* 2005, 17, 7–14.

(3) Law, M.; Goldberger, J.; Yang, P. D. *Ann. Rev. Mater. Res.* 2004, 34, 83–122.

(4) Schena, M.; Heller, R. A.; Theriault, T. P.; Konrad, K.; Lachenmeier, E.; Davis, R. W. *Trends Biotechnol.* 1998, 16, 301–306.

(5) Templin, M. F.; Stoll, D.; Schrenk, M.; Traub, P. C.; Vöhlinger, C. F.; Joos, T. O. *Trends Biotechnol.* 2002, 20, 160–166.

(6) Cui, Y.; Wei, Q.; Park, H.; Lieber, C. M. *Science* 2001, 293, 1289–1292.

(7) Gardeniers, J. G. E.; van den Berg, A. *Anal. Bioanal. Chem.* 2004, 378, 1700–1703.

(8) Neefjes, J.; Dantuma, N. P. *Nat. Rev. Drug Discuss.* 2004, 3, 58–69.

(9) LaVan, D. A.; McGuire, T.; Langer, R. *Nat. Biotechnol.* 2003, 21, 1184–1191.

(10) Bruno, F.; Pham, M. C.; DuBois, J. E. *Electrochim. Acta* 1997, 22, 451–457.

(11) Eddy, S.; Warriner, K.; Christie, I.; Ashworth, D.; Purkiss, C.; Vadgama, P. *Biosens. Bioelectron.* 1995, 10, 831–839.

(12) Long, D. D.; Marx, K. A.; Zhou, T. J. *Electroanal. Chem.* 2001, 501, 107–113.

(13) Pham, M. C.; DuBois, J.-E.; Lacaze, P.-C. *J. Electroanal. Chem.* 1979, 99, 331–340.

(14) DuBois, J.-E.; Lacaze, P.-C.; Pham, M. C. *J. Electroanal. Chem.* 1981, 117, 233–241.

(15) Situmorang, M.; Gooding, J. J.; Hibbert, D. B.; Barnett, D. *Biosens. Bioelectron.* 1998, 13, 953–962.

(16) Situmorang, M.; Gooding, J. J.; Hibbert, D. B. *Anal. Chim. Acta.* 1999, 394, 211–223.

(17) Yousaf, M. N.; Mrksich, M. *J. Am. Chem. Soc.* 1999, 121, 4286–4287.

(18) Curreli, M.; Li, C.; Sun, Y.; Lei, B.; Gundersen, M. A.; Thompson, M. E.; Zhou, C. *J. Am. Chem. Soc.* 2005, 127, 6922–6923.

(19) Bunimovich, Y. L.; Ge, G.; Beverly, K. C.; Ries, R. S.; Hood, L.; Heath, J. R. *Langmuir* 2004, 20, 10630–10638.

(20) Bartlett, P. N.; Cooper, J. M. *J. Electroanal. Chem.* 1993, 362, 1–12.

(21) Grosjean, L.; Cherif, B.; Mercey, E.; Roget, A.; Levy, Y.; Marche, P. N.; Villiers, M. B. *Anal. Biochem.* 2005, 347, 192–200.

(22) Szunerits, S.; Bouffier, L.; Calemczuk, R.; Corso, B.; Demeunynck, M.; Descamps, E.; Defontaine, Y.; Fiche, J. B.; Fortin, E.; Livache, T.; Mailley, P.; Roget, A.; Vieil, E. *Electroanalysis* 2005, 17, 2001–2017.

(23) Evans, S. A. G.; Brakha, K.; Billon, M.; Mailley, P.; Denuault, G. *Electrochem. Commun.* 2005, 7, 135–140.

(24) Bidan, G.; Billon, M.; Galasso, K.; Livache, T.; Mathis, C.; Roget, A.; Torres-Rodriguez, L. M.; Vieil, E. *Appl. Biochem. Biotechnol.* 2000, 89, 183–193.

(25) Kienle, S.; Lingler, S.; Kraas, W.; Offenhausser, A.; Knoll, W.; Jung, G. *Biosens. Bioelectron.* 1997, 12, 779–786.

ing<sup>10</sup> film is deposited on a conductive or semiconductive substrate. Two significant advantages of insulating films, such as polyphenols, are that they are considerably thinner due to the self-limiting nature of the polymerization reaction<sup>10,11,17</sup> and that substrates can be coated without affecting their electronic properties. The electropolymerization of tyramine and 4-hydroxybenzaldehyde has been shown to produce insulating films with reactive amines and aldehydes on bulk electrodes,<sup>13–16</sup> but the applications of this approach have been severely limited due to the lack of integration with thin-film microelectronic technology, which enables simultaneous functionalization of electrodes in large arrays with different molecular species.

In this article, we present a new method capable of applying multiple functionalities sequentially to interdigitated microelectrodes without the need for additional alignment steps and with no detectable cross-contamination. We demonstrate for the first time that modified phenols can be electrodeposited from aqueous solution onto lithographically patterned substrates to produce surfaces with free amine, aldehyde, and carboxylic acid groups capable of conjugating small molecules, proteins, and DNA oligonucleotides. In contrast with present electrochemical-based methods,<sup>26–28</sup> the power of the method introduced here is that it offers multiple conjugation chemistries, is not surface specific, is stable in aqueous environments, and is prepared entirely from commercially available chemicals. We additionally use indium tin oxide (ITO) electrodes in this study because ITO is optically transparent and useful for optical or fluorescent imaging applications.

## EXPERIMENTAL SECTION

**ITO Patterning.** Positive photoresist (ShIPLEY S1813) was spun on ITO slides (8–12  $\Omega \cdot \text{cm}$ ) purchased commercially (Sigma-Aldrich). The resist was patterned by contact photolithography (CAD Art Services transparency mask) and etched with TE-100 tin etchant (Transene).

**Electrode Preparation.** The reference electrode was fabricated by depositing AgCl on Ag wire (Earnest Fullham, Inc.) in an electrochemical cell from a saturated aqueous NaCl solution. The counter electrode is a Pt wire (Earnest Fullham, Inc.) and the working electrode was contacted with a Cascade Microprobe tip.

**Electrodepositions.** Tyramine, 4-hydroxybenzaldehyde, and 4-hydroxyphenylacetic acid were purchased at the highest available grade (Sigma-Aldrich) and used without further purification. The modified phenols were dissolved to 50 mM in 1 $\times$  phosphate-buffered saline (PBS), pH 7.4, using ultrasonication; fresh solutions were made at least every hour. Electropolymerization depositions on ITO were performed using a Gamry Femtostat by cycling the counter electrode voltage three times from 0.1 to  $-4$  V versus the reference electrode at a sweep rate of 100 mV/s. A comparison of depositions performed on bulk and patterned ITO shows that the peak current during deposition scales linearly with working electrode area. Following deposition, samples were washed with PBS and treated with this buffer with stirring for 15 min. Comparing depositions on bulk and patterned ITO, it is evident that the electropolymerization peak current scales linearly with

the working electrode surface area. Electrodepositions from 100 mM modified phenol in 0.1M KOH in methanol were performed for comparison, and results similar to those presented were obtained. It is important to note that nucleophilic R groups such as amines must be at least one carbon removed from the phenyl ring, or they will also polymerize and, hence, be rendered inactive.<sup>29</sup> It should also be noted that we have observed functional electropolymerized films created from 3-hydroxybenzaldehyde and 3-hydroxyphenylacetic acid. Though not studied in this work, ketone functionality can also be obtained by the electropolymerization of modified phenols.<sup>13</sup>

**Thickness Determinations.** Three thickness measurements were performed on each of five patterned samples, in which one lead had been coated by electrodeposition. These measurements were taken with a Tencor AlphaStep IQ surface profilometer, which has <5-nm step-height resolution. For each measurement, three leads were swept, with the coated lead located between two uncoated leads. The step heights are determined using the packaged software, which calculates the difference between the average height of the lead and that of the base flanking the lead. The step heights of the unfunctionalized leads are averaged and the thickness of the film is then calculated by subtracting this value from the step height of the functionalized lead. Of the 15 total measurements, none of which gave negative film thicknesses, four yielded film thicknesses of <5 nm, which is below the resolution of the profilometer.

**Blocking Measurements.** The solution for blocking measurements consists of 50 mM Fe<sup>2+</sup>/Fe<sup>3+</sup> in 0.1 M KCl. The blocking measurements were performed by sweeping from  $-0.5$  to  $0.5$  V versus the reference electrode at 500 mV/s 10 times; the tenth curve for each measurement is plotted in Figure 1F.

**Sample Washing.** Prior to all conjugation reactions, chips were rinsed three times with 1 $\times$  PBS and treated with this buffer for 15 min with agitation. Before imaging, each chip was rinsed with deionized water and blown dry with nitrogen gas. It should be noted that this drying procedure displaces the glass chips that fluoresce due to nonspecific binding.

**Amine Fluorescence Conjugation.** Samples were reacted with fluorophores (Molecular Probes) at 0.25 mg/mL in a pH 8.5 bicarbonate buffer at room temperature for 1 h with agitation. The red fluorophore is AlexaFluor 568 succinimidyl ester, and the blue is AlexaFluor 350 succinimidyl ester.

**Aldehyde and Carboxylic Acid Fluorescence Conjugation.** Samples were reacted with fluorophores at 0.25 mg/mL in a pH 5.5 acetate buffer for 1 h at room temperature with agitation. The fluorophore used to bind aldehyde was AlexaFluor 488 hydrazide, sodium salt, and that used to bind carboxylic acid was AlexaFluor 568 hydrazide, sodium salt. The amine-coated slide used as a positive control was purchased from BioSlide, Inc.

**Amine Quantification.** Slide surface free amine quantification was performed based on a serially diluted lysine standard run in triplicate; bound *o*-phthaldialdehyde (Sigma) was excited at 360 nm and the fluorescence was measured at 460 nm.

**Amine and Aldehyde Quenching.** Amine-coated samples were treated with 0.1 M sulfo-*N*-hydroxysuccinimide (NHS) in pH 8.3 bicarbonate for 1 h at room temperature with agitation for

(26) Konry, T.; Novoa, A.; Cosnier, S.; Marks, R. S. *Anal. Chem.* **2003**, *75*, 2633–2639.

(27) Cosnier, S. *Anal. Bioanal. Chem.* **2003**, *377*, 507–520.

(28) Adamcova, Z.; Ludmila, D. *Prog. Org. Coat.* **1989**, *16*, 295–320.

(29) Guenbour, A.; Kacemi, A.; Benbachir, A. *Prog. Org. Coat.* **2000**, *39*, 151–155.

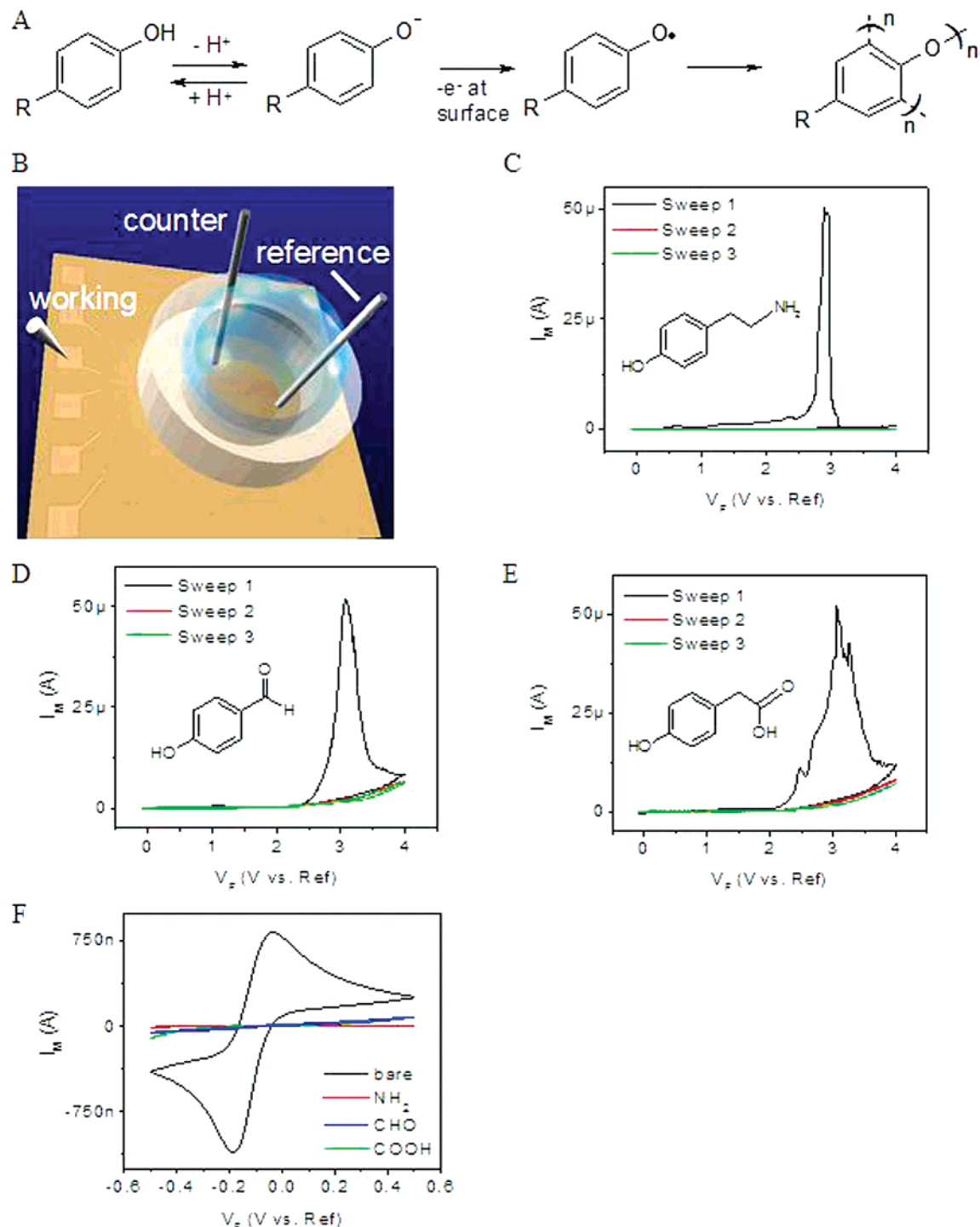


**Figure 1.** (A) Schematic of surface electrochemical polymerization. R = (CH<sub>2</sub>)<sub>2</sub>NH<sub>2</sub>, CHO, and CH<sub>2</sub>COOH for tyramine, 4-hydroxybenzaldehyde, and 4-hydroxyphenylacetic acid, respectively. (B) Schematic (not to scale) of an electrochemical cell defined by a PDMS gasket on a patterned ITO-on-glass substrate. (C) Cyclic voltammogram of the electropolymerization of tyramine (inset) on a single patterned ITO lead on a glass substrate (Figure 1B). The current measured at the working electrode,  $I_M$ , is plotted versus the forced voltage between the counter and reference electrodes,  $V_F$ . The potential at which the oxidation occurs is strongly dependent on (i) the working electrode material and (ii) the freshness of the reference electrode (the peak has been seen to occur between  $\sim 2.4$  and  $3.25$  V on ITO). (D) Cyclic voltammogram of 4-hydroxybenzaldehyde (inset) electrodeposition on a patterned ITO lead. (E) Cyclic voltammogram of 4-hydroxyphenylacetic acid (inset) electrodeposition on a patterned ITO lead. (F) Cyclic voltammogram of the blocking solution on bare ITO, polytyramine-coated ITO (NH<sub>2</sub>), poly(4-hydroxybenzaldehyde)-coated ITO (CHO), and poly(4-hydroxyphenylacetic acid)-coated ITO (COOH). The measurements were taken with the same cell used for deposition. The reduction and oxidation peaks are not symmetric about 0 V due to coating of the reference electrode. All experiments were repeated over 20 times with similar results.

quenching. Aldehyde-coated samples were quenched with 0.1 M hydrazine in pH 6.5 acetate buffer for 1 h at room temperature with agitation.

**Carbodiimide Coupling, Antibody Binding, and Oligonucleotide Hybridization.** Carboxylic acid groups (either on bovine serum albumin (BSA) or bound to ITO) were treated with

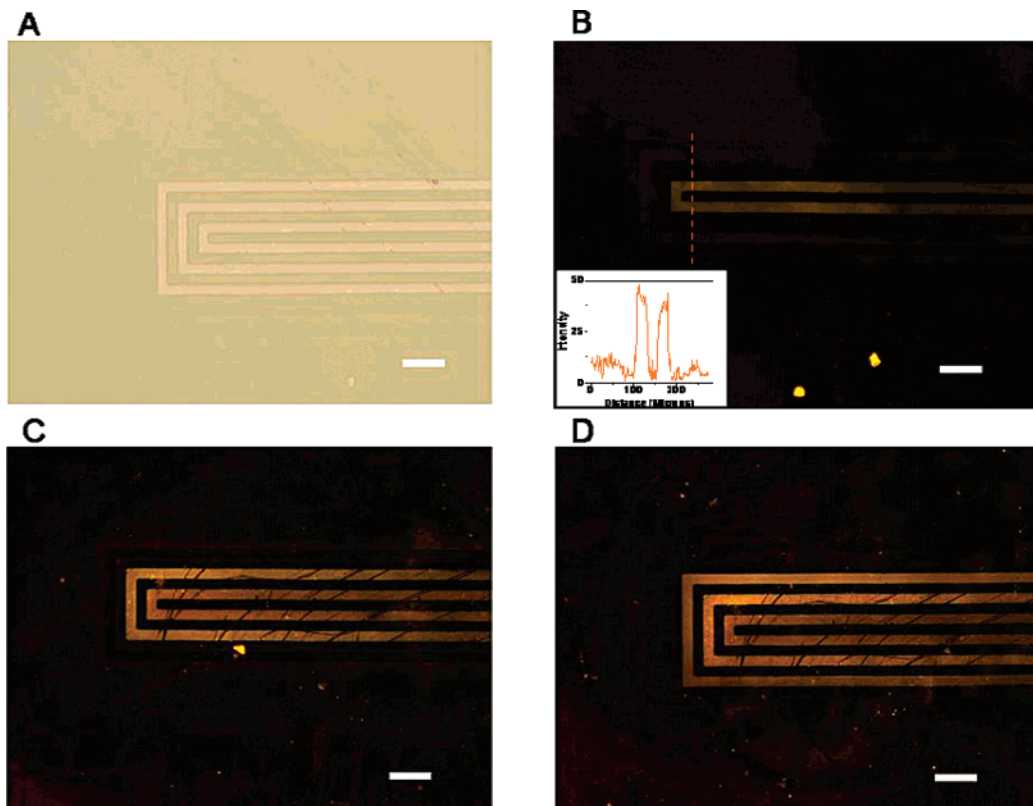


**Figure 2.** (A) Bright-field image showing the three parallel “C-shaped” ITO leads. Treatment with a red, amine-reactive fluorophore and subsequent fluorescence imaging at this stage (TRITC filter) showed no specific binding (not shown). (B) Fluorescence image (TRITC filter) of the chip shown in (A) with the inner lead coated with polytyramine and subsequently reacted with a red amine-reactive fluorophore. The inset plot shows the fluorescence intensity (determined with arbitrary units defined by ImageJ) versus distance for the orange outline. Leads functionalized with amines and subsequently quenched exhibited no specific fluorescence pattern when treated with the same fluorophore. (C) Fluorescence image (TRITC filter) of the chip shown in (B) with the middle lead now coated with polytyramine and a subsequent reaction with the same dye. Visible scratches were purposely introduced at this stage (with tweezers) to register sample identity. (D) Same as (C) but with the outermost lead also coated with polytyramine and reacted with the same dye. The scratch patterns in (C) and (D) are identical. The white scale bar in all images represents  $100\ \mu\text{m}$ . The experiment was repeated four times with similar results. The average intensity of the fluorescent signal across the  $25\text{-}\mu\text{m}$  leads for the four experiments was  $37 \pm 4$  over a background of  $8 \pm 5$ .

$0.015\ \text{M}$  1-ethyl-3-(3-dimethylaminopropyl)carbodiimide (EDC) and  $0.03\ \text{M}$  NHS at pH 5.5, and amine groups were treated with pH 9.5 buffer for 15 min at room temperature with agitation. The solutions were then combined and left for 1 h at room temperature with agitation. The final BSA concentration was  $1\ \text{mg/mL}$ . It should be noted that NHS and EDC are not required for the amine–aldehyde reaction of the DNA 20-mer conjugation. Antibody binding was performed in  $1\times$  PBS at  $37\ ^\circ\text{C}$  for 1 h at a concentration of  $100\ \mu\text{g/mL}$ . Oligonucleotide hybridization was performed at a concentration of  $50\ \mu\text{M}$  in  $1\times$  SCC buffer (pH 7.2) with 0.05% sodium dodecyl sulfate at room temperature for 30 min with agitation.

**DNA Oligonucleotide Sequences.** The amino-terminated DNA 20-mer sequence was  $5\text{-H}_2\text{N-CGCCACTGCGTCACTG-CAGG-3}'$  and the fluorescently labeled sequence was  $5\text{-FAM-CCTGCAGTGACGCAGTGGCG-3}'$  (IDT, Inc.).

**BSA Quantification.** The bound BSA concentration was quantified with an absorbance measurement at 562 nm using a micro bicinchoninic acid (BCA) protein assay kit (Pierce) based on a serially diluted BSA standard run in triplicate.

## RESULTS AND DISCUSSION

The deposition solution is created by dissolving a substituted phenol in PBS (Figure 1A). This is subsequently loaded into an

electrochemical cell defined by a poly(dimethylsiloxane) (PDMS) gasket (Figure 1B). Voltage is then cycled between the counter and reference electrodes, while current is measured at the working electrode (the patterned surface in Figure 1B, which fans out to a contact pad that can be accessed and electrically contacted by a microprobe). The insulating surface coating is produced by a free radical polymerization, which has previously been reported to occur at the ortho positions of the ring,<sup>12</sup> in which free radicals are generated by the removal of an electron from deprotonated phenyl rings at the working electrode.

The electropolymerization of tyramine at the working electrode, a patterned ITO lead, is evident from the presence of a strong oxidation peak of  $\sim 50\ \mu\text{A}$  during the first sweep in the cyclic voltammogram in Figure 1C (for an electrode of  $\sim 1.53 \times 10^5\ \mu\text{m}^2$ , the current density is  $\sim 0.29\ \text{nA}/\mu\text{m}^2$ ). The absence of this peak from subsequent sweeps indicates that tyramine oxidation is nonreversible and self-limiting. The deposition of this insulating coating has a minimal effect on electrode conductivity. Panels D and E in Figure 1 show the cyclic voltammograms for the electropolymerizations of 4-benzaldehyde and 4-hydroxyphenylacetic acid, respectively. Film thickness was determined by profilometry to be between  $<5$  (the resolution of the profilometer) and  $30\ \text{nm}$  across 15 measurements (three on each of five



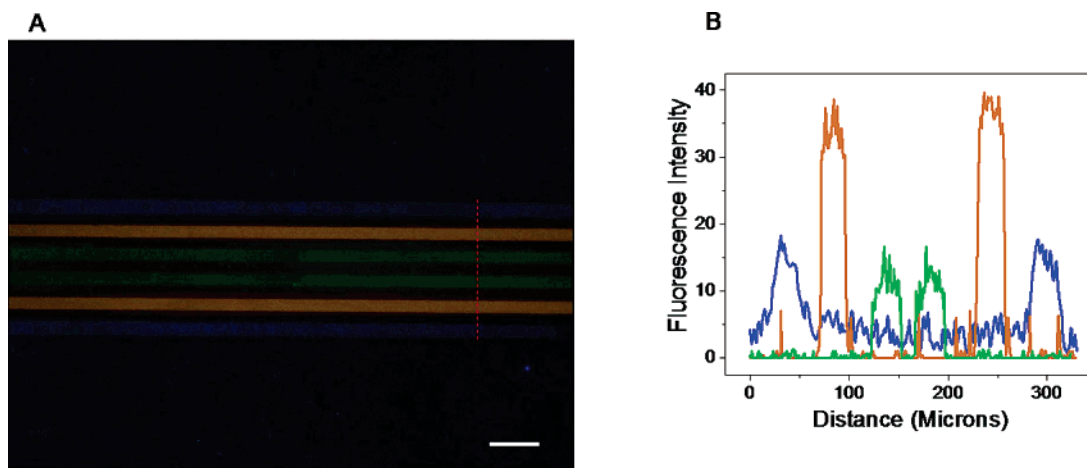


**Figure 3.** (A) Multiple-fluorescence (DAPI, GFP, and TRITC filters) image of a central part of the lead pattern for a sample treated as follows. Polytyramine was deposited on the outermost lead and the chip was subsequently treated with a blue, amine-reactive fluorophore. Poly(4-hydroxybenzene) was then deposited on the innermost lead, followed by chip treatment with a green, aldehyde-reactive fluorophore. Free aldehyde groups were then quenched. Last, poly(4-hydroxyphenylacetic acid) was deposited on the middle lead and the chip was treated with a red, carboxylic acid-reactive fluorophore. The scale bar represents 100  $\mu\text{m}$ . The three individual filtered images were merged to give the figure shown. (B) Fluorescence intensity versus position for the red cut line in (A). The line color corresponds to the fluorescence color in (A); the fluorescence intensity units are defined by ImageJ. The experiment was repeated three times with similar results.

samples), with an average of  $15 \pm 6$  nm, lower than that reported previously.<sup>14</sup> This variation is expected as film thickness can be tuned by the sweep rate, the extent of the forced voltage, and the number of sweeps performed to achieve the thinner values desirable for semiconductor sensing applications or thicker values required to prevent metal corrosion without affecting functionalization.

The insulating nature of the films was evaluated by performing blocking measurements with an iron(II)/iron(III) redox couple (Figure 1F). For comparison, cyclic voltammetry with this solution was first performed on a bare ITO surface and substantial oxidation and reduction peaks due to the conducting substrate are evident. These peaks are not apparent in blocking measurements performed after film deposition, consistent with the deposition of an insulating (polyphenol) film on the working electrode. The residual current present in these sweeps can be attributed mainly to tunneling through the polyphenol film.<sup>30</sup>

We first demonstrate the ability of this method to selectively and sequentially functionalize patterned electrodes. A bright-field image of the edge of the lead pattern on a representative substrate (Figure 2A) shows three 25- $\mu\text{m}$ -wide, electrically isolated and interdigitated “C-shaped” leads that fan out to contact pads (not shown). A PDMS gasket was placed around all the leads to create an electrochemical cell (as depicted in Figure 1B). Only one lead was used as the working electrode (here, the innermost lead), and its surface was selectively functionalized with amine groups by tyramine electropolymerization as described previously. The sample was then exposed to a red, amine-reactive fluorophore, and the fluorescence micrograph in Figure 2B demonstrates that amines were selectively introduced as a result of the electropolymerization. The inset plot of the fluorescence intensity shows that the amines are solely detectable on the innermost lead. A subsequent tyramine electrodeposition was performed on the

middle lead, and the sample was treated with the same amine-reactive fluorophore and imaged; both the innermost and middle leads now fluoresce (Figure 2C). The electropolymerization/fluorescence conjugation was then performed on the outermost lead, and the fluorescence micrograph in Figure 2D shows all leads fluorescing, indicative of the third selective deposition. The stability of the coating does not appear to be a problem as the fluorescence remains visible for at least six months after functionalization for samples stored in air.

For scalability, it is crucial to know the packing density of amine groups on the surface of the electropolymerized film. The presence of amines on bulk ITO substrates was quantified with an *o*-phthaldialdehyde assay.<sup>31</sup> We found that there were  $3.1 \pm 0.7$  free amines/ $\text{nm}^2$ , which was in good agreement with the density of amine surfaces formed by closest-packed self-assembled monolayers in the literature<sup>32</sup> and on a commercially available amine-coated slide that was used as a positive control and showed  $2.7 \pm 0.4$  available amines/ $\text{nm}^2$ .

To demonstrate the versatility and generality of this technique, we derivatized each of the three leads sequentially with different functional groups and then conjugated different moieties onto each group. As before, a PDMS gasket was placed around all the leads for each of the following depositions. First, the outermost lead was functionalized with amine (as described previously) and treated with a blue, amine-reactive fluorophore. Second, the innermost electrode was functionalized with aldehyde by 4-hydroxybenzaldehyde electrodeposition, followed by binding of a green, aldehyde-reactive fluorophore. After quenching remaining aldehyde groups with hydrazine, the middle lead was functionalized with carboxylic acid by 4-hydroxyphenylacetic acid electrodeposition. A red, carboxylic acid-reactive fluorophore was subsequently conjugated to the surface and the sample was then imaged; the fluorescence micrograph is shown in Figure 3A and

(30) Gao, Z.; Siow, K. S. *Electrochim. Acta* **1997**, *42*, 315–321.

(31) Buck, R. H.; Krummen, K. J. *Chromatogr.* **1987**, *387*, 255–265.

(32) Lateef, S. S.; Boateng, S.; Ahluwalia, N.; Hartman, T. J.; Russell, B.; Hanley, L. J. *Biomed. Mater. Res., A* **2005**, *72*, 373–380.

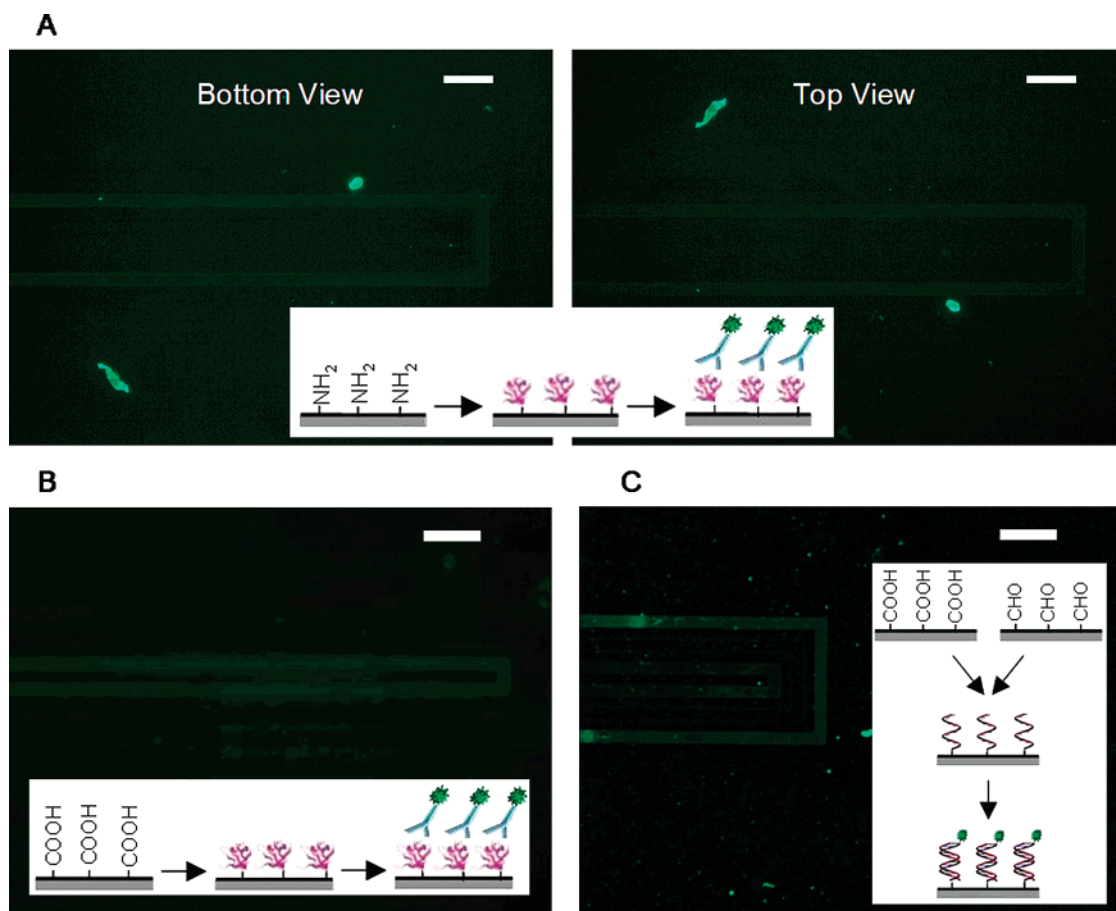


**Figure 4.** (A) Fluorescence micrograph of the end of an electrode pattern first coated with polytyramine, then carbodiimide coupled to BSA, and last incubated with a fluorescently labeled BSA IgG, as illustrated by the schematic inset. The “bottom view” is immunofluorescence viewed through the ITO; the “top view” is the immunofluorescence viewed directly, illustrating the transparency of ITO. When the  $\alpha$ -BSA IgG was replaced with a nonimmune, fluorescently labeled IgG from the same species and at the same concentration, or when BSA was not bound on the surface prior to  $\alpha$ -BSA-FITC IgG incubation, no specific immunofluorescence pattern was observed (not shown). (B) Fluorescence micrograph of the lead pattern with the innermost lead first coated with poly(4-hydroxyphenylacetic acid) and then treated as in (A) (schematic inset). (C) Fluorescence micrograph of a patterned substrate coated with poly(4-hydroxybenzaldehyde) on the innermost leads and poly(4-hydroxyphenylacetic acid) on the outermost leads. Subsequently, carbodiimide coupling was performed to an amino-terminated DNA 20-mer, followed by hybridization using a fluorescently labeled complementary 20-mer and subsequent fluorescence imaging. When a noncomplementary DNA 20-mer was used for hybridization at the same concentration or when DNA was not immobilized on the lead surface prior to probe hybridization, no specific fluorescence was observed (not shown). All fluorescent images were taken with a GFP filter, and the scale bar in each micrograph represents 100  $\mu\text{m}$ . All experiments were repeated four times with similar results.

the localization of each of the three fluorophores is apparent. The fluorescence intensity plot in Figure 3B demonstrates the absence of cross-functionalization (i.e., nonspecific) interaction.

A key feature of this approach is the ability to selectively bind targets arrayed on the substrate. To demonstrate this feature, we studied the localization of a protein, BSA, and a DNA oligonucleotide to the functionalized surfaces. Amine and carboxylic acid groups are desirable for protein conjugation,<sup>33</sup> while aldehyde and carboxylic acid groups are preferred for DNA binding.<sup>34</sup> A carbodiimide coupling reaction was utilized to conjugate BSA to the central leads of a chip functionalized with amines. The sample was subsequently incubated with chicken  $\alpha$ -BSA-FITC (green fluorescence) immunoglobulin G (IgG) antibody and the fluorescence micrograph of the sample is shown in Figure 4A. A second

sample was electrodeposited with poly(4-hydroxyphenylacetic acid) on the innermost lead and then subjected to a similar treatment; the fluorescence micrograph is shown in Figure 4B. The fluorescent intensity in both samples is localized to the functionalized lead, illustrating the conjugation of BSA to the surface and the subsequent BSA- $\alpha$ -BSA-FITC IgG binding. Surface-conjugated BSA density was determined with a BCA assay<sup>35</sup> to be  $4.2 \pm 0.6$  molecules/100 nm<sup>2</sup> on bulk ITO substrates, which is reasonable given the  $\sim 25\text{-nm}^2$  footprint of the protein.

To study the binding of DNA oligonucleotides to the electropolymerized surfaces, a third sample was functionalized with carboxylic acid on the outermost and aldehyde on the innermost lead. A 5'-amine-terminated DNA 20-mer was conjugated to the surface under conditions similar for BSA conjugation. The sample was subsequently treated with a complementary DNA 20-mer

(33) Hermanson, G. T. *Bioconjugate Techniques*; Academic Press: New York, 1996.

(34) Taylor, S.; Smith, S.; Windle, B.; Guiseppi-Elie, A. *Nucleic Acids Res.* **2003**, *31*, e87.

(35) Smith, P. K.; Krohn, R. I.; Hermanson, G. T.; Mallia, A. K.; Gartner, F. H.; Provenzano, M. D.; Fujimoto, E. K.; Goeke, N. M.; Olson, B. J.; Klenk, D. C. *Anal. Biochem.* **1985**, *150*, 76–85.

labeled with a 5'-FAM (green fluorescence) and fluorescently imaged (Figure 4C). Both functionalized leads fluoresce, demonstrating DNA conjugation to each surface and subsequent hybridization with the fluorescent DNA probe.

## CONCLUSION

To our knowledge, this is the first demonstration of a selective-coating electrochemical approach that can be successfully tuned to a wide range of functionalizations. We have demonstrated site-specific conjugation of small molecules, proteins, and DNA oligonucleotides to surface amine, aldehyde, and carboxylic acid groups on insulating films electrodeposited on prepatterned electrodes. With this approach, electrically conducting and semiconducting materials of any lithographic geometry are capable of being selectively functionalized without additional alignment steps. This in situ alignment allows for scaling to nanodevices due to the high density of functional groups on the film surface. Thus, the sequential deposition of numerous chemical or biochemical species of interest at high density on a surface with minimal cross-contamination is realizable. This approach has many potential applications, including selective sensor coating, higher density genomic and DNA arraying, lower volume drug discovery and forensic analyses platforms, and selective coatings for patterning

micro- and nanoenvironments for lab-on-a-chip and other microfluidic, microchannel, and MEMS applications.

## ACKNOWLEDGMENT

The authors thank James Klemic for many helpful discussions and assistance with manuscript preparation; Alec Flyer, Pauline Wyrembak, Elnaz Menhaji, and Kathryn Klemic for many helpful discussions and experimental suggestions; David Stern for help preparing the manuscript; Millicent Ford for assistance with fluorescence microscopy; Menno de Jong for assistance designing the electrochemical cell; Russel, Nicholas, and Vincent Bernando for help with the design and machining of the electrochemical cell; and Fred Sigworth, Ron Breaker, Mark Saltzman, and Erin Lavik for helpful discussions about fluorescence detection. This work was partially supported by DARPA through AFOSR (FA9550-05-1-0395) and ONR (N66001-04-1-8902), NASA (NCC 2-1363), by a Department of Homeland Security graduate fellowship, and by a NSF graduate fellowship.

Received for review March 6, 2006. Accepted June 27, 2006.

AC060410R